

Excited-State Half-Lives in ^{130}Cd and the Isospin Dependence of Effective Charges

A. Jungclaus,¹ M. Górska,² M. Mikołajczuk,^{2,3} J. Acosta,¹ J. Taprogge,^{1,4,5} S. Nishimura,⁵ P. Doornenbal,⁵ G. Lorusso,⁵ G. S. Simpson,⁶ P.-A. Söderström,^{5,*} T. Sumikama,⁷ Z. Xu,⁸ P. Kumar,^{9,2} G. Martínez-Pinedo,^{2,9} F. Nowacki,¹⁰ P. Van Isacker,¹¹ H. Baba,⁵ F. Browne,^{12,5} N. Fukuda,⁵ R. Gernhäuser,¹³ G. Gey,^{6,14,5} N. Inabe,⁵ T. Isobe,⁵ H. S. Jung,^{15,†} D. Kameda,⁵ G. D. Kim,¹⁶ Y.-K. Kim,^{16,17} I. Kojouharov,² T. Kubo,⁵ N. Kurz,² Y. K. Kwon,¹⁶ Z. Li,¹⁸ H. Sakurai,^{5,8} H. Schaffner,² Y. Shimizu,⁵ K. Steiger,¹³ H. Suzuki,⁵ H. Takeda,⁵ Zs. Vajta,^{19,5} H. Watanabe,⁵ J. Wu,^{18,5} A. Yagi,²⁰ K. Yoshinaga,²¹ G. Benzoni,²² S. Bönig,²³ K. Y. Chae,²⁴ J.-M. Daugas,²⁵ F. Drouet,⁶ A. Gadea,²⁶ S. Ilieva,²³ F. G. Kondev,²⁷ T. Kröll,²³ G. J. Lane,²⁸ A. Montaner-Pizá,²⁶ K. Moschner,²⁹ F. Naqvi,³⁰ M. Niikura,⁸ H. Nishibata,²⁰ A. Odahara,²⁰ R. Orlandi,^{31,32} Z. Patel,³³ Zs. Podolyák,³³ and A. Wendt²⁹

¹Instituto de Estructura de la Materia, CSIC, E-28006 Madrid, Spain

²GSII Helmholtzzentrum für Schwerionenforschung, D-64291 Darmstadt, Germany

³Faculty of Physics, University of Warsaw, Warsaw, PL-02093, Poland

⁴Departamento de Física Teórica, Universidad Autónoma de Madrid, E-28049 Madrid, Spain

⁵RIKEN Nishina Center, RIKEN, 2-1 Hirosawa, Wako-shi, Saitama 351-0198, Japan

⁶LPSC, Université Joseph Fourier Grenoble 1, CNRS/IN2P3, Institut National Polytechnique de Grenoble, F-38026 Grenoble Cedex, France

⁷Department of Physics, Tohoku University, Aoba, Sendai, Miyagi 980-8578, Japan

⁸Department of Physics, University of Tokyo, Hongo 7-3-1, Bunkyo-ku, 113-0033 Tokyo, Japan

⁹Institut für Kernphysik (Theoriezentrum), Fachbereich Physik, Technische Universität Darmstadt, D-64289 Darmstadt, Germany

¹⁰Université de Strasbourg, CNRS, IPHC UMR, Strasbourg, 7178, F-67000, France

¹¹Grand Accélérateur National d'Ions Lourds, CEA/DRF-CNRS/IN2P3, F-14076 Caen, France

¹²School of Computing, Engineering and Mathematics, University of Brighton, Brighton BN2 4GJ, United Kingdom

¹³Physik Department E12, Technische Universität München, D-85748 Garching, Germany

¹⁴Institut Laue-Langevin, B.P. 156, F-38042 Grenoble Cedex 9, France

¹⁵Department of Physics, Chung-Ang University, Seoul 156-756, Republic of Korea

¹⁶Rare Isotope Science Project, Institute for Basic Science, Daejeon 305-811, Republic of Korea

¹⁷Department of Nuclear Engineering, Hanyang University, Seoul 133-791, Republic of Korea

¹⁸School of Physics and State key Laboratory of Nuclear Physics and Technology, Peking University, Beijing 100871, China

¹⁹MTA Atomki, P.O. Box 51, Debrecen H-4001, Hungary

²⁰Department of Physics, Osaka University, Machikaneyama-machi 1-1, Osaka 560-0043 Toyonaka, Japan

²¹Department of Physics, Faculty of Science and Technology, Tokyo University of Science, 2641 Yamazaki, Noda, Chiba, Japan

²²INFN, Sezione di Milano, via Celoria 16, I-20133 Milano, Italy

²³Institut für Kernphysik, Technische Universität Darmstadt, D-64289 Darmstadt, Germany

²⁴Department of Physics, Sungkyunkwan University, Suwon 440-746, Republic of Korea

²⁵CEA, DAM, DIF, F-91297 Arpaçon cedex, France

²⁶Instituto de Física Corpuscular, CSIC-Univ. of Valencia, E-46980 Paterna, Spain

²⁷Physics Division, Argonne National Laboratory, Lemont, Illinois 60439, USA

²⁸Department of Nuclear Physics, Research School of Physical Sciences and Engineering, Australian National University, Canberra, Australian Capital Territory 0200, Australia

²⁹IKP, University of Cologne, D-50937 Cologne, Germany

³⁰Wright Nuclear Structure Laboratory, Yale University, New Haven, Connecticut 06520-8120, USA

³¹Instituut voor Kern- en StralingsFysica, K.U. Leuven, B-3001 Heverlee, Belgium

³²Advanced Science Research Center, Japan Atomic Energy Agency, Tokai, Ibaraki, 319-1195, Japan

³³Department of Physics, University of Surrey, Guildford GU2 7XH, United Kingdom



(Received 6 November 2023; revised 21 February 2024; accepted 18 April 2024; published 29 May 2024)

The known $I^\pi = 8_1^+$, $E_x = 2129$ -keV isomer in the semimagic nucleus $^{130}\text{Cd}_{82}$ was populated in the projectile fission of a ^{238}U beam at the Radioactive Isotope Beam Factory at RIKEN. The high counting statistics of the accumulated data allowed us to determine the excitation energy, $E_x = 2001.2(7)$ keV, and half-life, $T_{1/2} = 57(3)$ ns, of the $I^\pi = 6_1^+$ state based on $\gamma\gamma$ coincidence information. Furthermore, the half-life of the 8_1^+ state, $T_{1/2} = 224(4)$ ns, was remeasured with high precision. The new experimental information, combined with available data for ^{134}Sn and large-scale shell model calculations, allowed us to

extract proton and neutron effective charges for ^{132}Sn , a doubly magic nucleus far-off stability. A comparison to analogous information for ^{100}Sn provides first reliable information regarding the isospin dependence of the isoscalar and isovector effective charges in heavy nuclei.

DOI: 10.1103/PhysRevLett.132.222501

The concept of effective nucleon charges was introduced in many nuclear models in order to compensate for the neglect of the coupling of the electromagnetic operator to nucleons outside the considered valence space [1–4]. In the nuclear shell model (SM), effective nucleon-nucleon interactions among the valence nucleons are employed to calculate the energies of excited states and effective charges, i.e., charges which include renormalization corrections to the bare charges of both protons and neutrons, are used in the calculation of electromagnetic transition probabilities. As illustrated in Fig. 1, the quadrupole response of atomic nuclei mainly consists of two components, namely, (i) particle-hole excitations among single-particle orbitals close to the Fermi surface, i.e., within the same harmonic oscillator shell ($\Delta n = 0$, with n the major oscillator quantum number), and (ii) particle-hole excitations to the next harmonic oscillator shell with the same

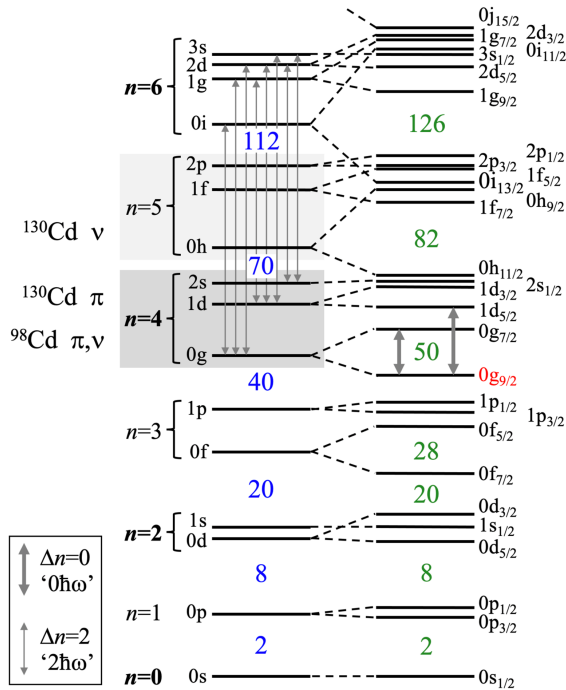


FIG. 1. Sketch of the single-particle orbitals and shell gaps considering the harmonic oscillator potential, left, and adding the ℓ^2 and spin-orbit terms, right (adopted from Ref. [7]). The $n = 4$ (even n in bold correspond to positive parity) and $n = 5$ (odd n correspond to negative parity) harmonic oscillator shells considered as valence spaces in the present SM calculations are shown as gray boxes. Thick (thin) gray arrows indicate $\Delta n = 0$ ($\Delta n = 2$) particle-hole excitations of the doubly magic nucleus ^{100}Sn .

parity, i.e., $\Delta n = 2$. While the first give rise to discrete 2^+ states with excitation energies of up to a few MeV, the latter correspond to the giant quadrupole resonances (GQRs) observed at significantly higher energies (roughly $E_x \approx 2\hbar\omega$, e.g., ≈ 16 – 17 MeV for $^{100,132}\text{Sn}$ [5,6]). In SM calculations considering a full harmonic oscillator shell as valence space for both protons and neutrons (commonly called $0\hbar\omega$ calculations), the effective charges therefore compensate for the nonconsideration of virtual excitations of the isoscalar and isovector GQR.

A first general estimate of the isoscalar and isovector effective charges and their dependence on the neutron excess based on the collective model was presented by Bohr and Mottelson [8]. When phenomenological interactions are used, the effective charges are usually adjusted to available experimental data. For electric quadrupole transitions in the sd and pf valence spaces corresponding to the $n = 2$ and $n = 3$ harmonic oscillator shells, typically values around $e_\pi = 1.4$ – $1.5e$ and $e_\nu = 0.5e$ were determined [9–12] indicating that the effect of polarization is similar for both neutrons and protons, i.e., isovector contributions to the effective charges are small. However, the use of constant effective charges for a given model space is only an approximation since they are expected to depend on both the single-particle quantum numbers of the initial and final states as well as the isospin. Orbital-dependent effective charges were calculated for many nuclei and using a variety of different theoretical approaches [13–18], but only recently both effective interactions and effective charges were microscopically derived in a consistent way [19,20]. On the experimental side, it is very difficult to disentangle the effects of these two dependencies. In the pf shell, for example, very different (e_π , e_ν) values were extracted from measured transition rates between high-spin states dominated by the $0f_{7/2}$ orbital in the $A = 51$ mirror nuclei $^{51}\text{Fe}/^{51}\text{Mn}$, i.e., close to $N = Z$ [21], as compared to those determined based on $0p_{3/2}$ dominated states in the $N = 30$ isotones ^{50}Ca and ^{51}Sc ($N/Z = 1.50/1.43$) [22]. Since the two cases differ in both the isospin and the dominant single-particle orbital, no conclusion can be drawn regarding the dependence of the effective charges on these two parameters.

In order to study the isospin dependence of the effective charges without orbital effects, transitions between states with the same pure configuration in two nuclei with very different proton-to-neutron ratio have to be studied. Such a clean laboratory is offered by the two semimagic Cd isotopes ^{98}Cd and ^{130}Cd ($Z = 48$). In all calculations

performed within the $Z = 28\text{--}50$ proton shell, they feature excited states of exceptionally pure structure, namely, the 8^+ , 6^+ (both 100%), and 4^+ ($> 99\%$) members of the $\pi 0g_{9/2}^{-2}$ multiplet, and span the entire $N = 50\text{--}82$ major neutron shell, reaching from $N \approx Z$ to the very neutron-rich side of the nuclear chart ($N/Z = 1.71$). Note that $^{98,130}\text{Cd}$ is the only pair of semimagic isotopes or isotones with two nucleons or two holes outside a jj -closed doubly magic core that currently is available for such a study. Furthermore, the purity of the first excited states in these nuclei, which has its origin in the isolated position of the high- j $0g_{9/2}$ intruder orbital in the $N = 28\text{--}50$ shell, is unique. Experimentally determined half-lives of the 8^+ and 6^+ states in ^{98}Cd were already presented in Ref. [23]. Here, we report on high precision measurements of the corresponding half-lives in ^{130}Cd . In combination with new large-scale shell model (LSSM) calculations, these experimental results allow us for the first time to trace the isospin dependence of the $E2$ effective charges in heavy nuclei.

The experiment was performed at the Radioactive Isotope Beam Factory (RIBF) of the RIKEN Nishina Center within the EURICA campaign. The neutron-rich ^{130}Cd nuclei were produced following the projectile fission of a 345-MeV/ u ^{238}U beam with an average intensity of about 8 pnA, impinging on a 3-mm thick Be target. The ions of interest were identified on an ion-by-ion basis by means of the BigRIPS in-flight separator (BR) [24] using the ΔE -TOF- $B\rho$ method [25]. Further information about the identification procedure is provided in Ref. [26] which reports on the β decay of ^{130}Cd based on the same dataset. In total about 1.8×10^6 ^{130}Cd ions were identified and implanted into the WAS3ABi (Wide-range Active Silicon Strip Stopper Array for β and ion detection) Si array [27,28] positioned at the focal plane of the ZeroDegree (ZD) spectrometer [24]. Following the fission reaction, some of the fragments are populated in isomeric states with half-lives long enough to survive the flight time through the BR and ZD spectrometers. To detect the delayed γ radiation emitted following the decay of these isomeric states after the implantation of the fragments in the Si array, 12 large-volume Ge Cluster detectors [29] from the former EUROBALL spectrometer [30] were arranged in a close geometry around the WAS3ABi detector.

A spectrum of γ rays observed in delayed coincidence with identified and implanted ^{130}Cd ions is shown in Fig. 2(a). Four transitions with energies of 127.4(2), 137.6(2), 538.6(3), and 1325.0(6) keV, respectively, are clearly visible, in full agreement with the observation reported in Ref. [31]. In that work, these transitions were assigned to form an $E2$ cascade from an 8^+ isomer with a half-life of $T_{1/2} = 220(30)$ ns to the ground state, although it was not possible to decide which of the two low-energy γ rays corresponds to the primary isomeric decay. Thanks to the considerably higher counting statistics accumulated

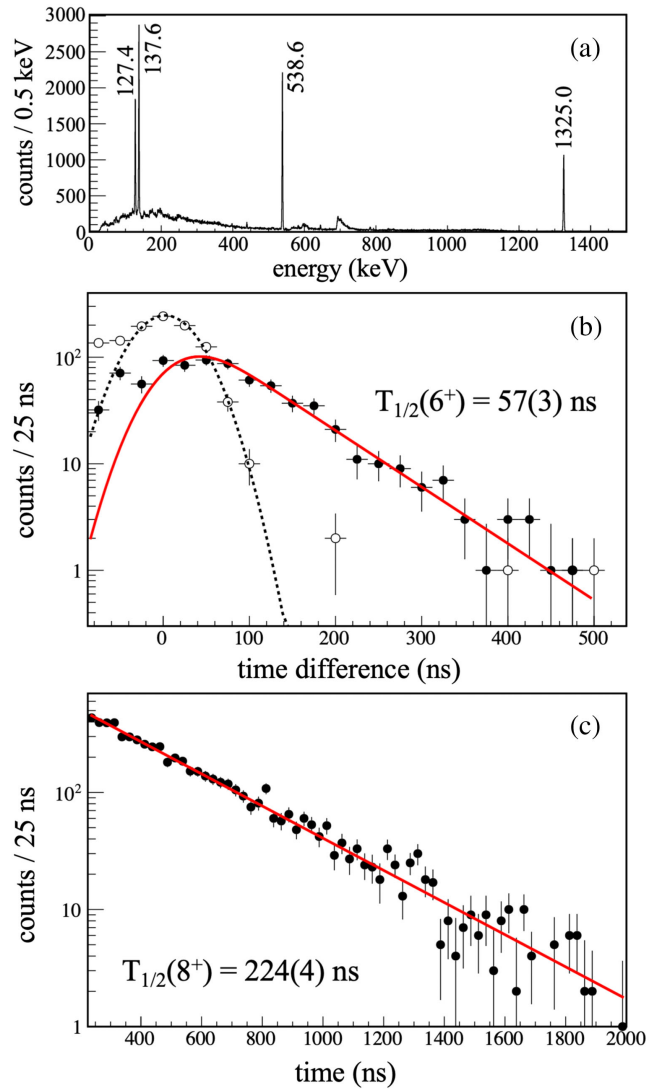


FIG. 2. (a) Delayed γ -ray spectrum ($t = 75$ ns– 2 μ s) in coincidence with ^{130}Cd ions implanted in WAS3ABi. (b) Time-difference distributions of the 127.4- (filled circles) and 137.6-keV (open circles) γ rays as start and the 538.6-keV/1325.0-keV transitions as stop and (c) time distribution of the 127.4-keV γ ray fitted by a single exponential decay (red line).

in the present experiment, the order between the two low-energy transitions could now be firmly established on the basis of excited-state lifetime information. Time-difference spectra were sorted for each pair among the four observed transitions. No delay is observed between the detection of the 538.6-keV, $4^+ \rightarrow 2^+$ and 1325.0-keV, $2^+ \rightarrow 0^+$ transitions, in agreement with the expectation of a lifetime of the 2^+ state in the subnanosecond range. Therefore, both these transitions are equally well suited to construct the time-difference distributions for the two low-energy γ rays. The summed distributions, with either the 538.6- or the 1325.0-keV transition as stop, are shown in Fig. 2(b). Obviously, the two distributions exhibit a very different temporal behavior. While the time difference

between the 538.6-keV/1325.0-keV γ rays and the 137.6-keV transition is well described by a Gaussian distribution with a width which reflects the time resolution of the Ge detectors, the one for the 127.4-keV transition clearly features an exponential decay component. This finding allows us to unequivocally assign the 127.4-keV transition to decay from the 8^+ and the 137.6-keV transition from the 6^+ state and thus to fix the excitation energy of the 6^+ state to $E_x(6^+) = 2001.2(7)$ keV. To determine the half-life of the 6^+ state, a likelihood fit of the time-difference distribution between the 127.4-keV γ ray and the two high-energy transitions shown in Fig. 2(b) was performed with an exponentially modified Gaussian in which the width of the Gaussian was fixed to the value obtained from a fit of the distribution of the 137.6-keV transition. This analysis yielded a value of $T_{1/2}(6^+) = 57(3)$ ns, which is in perfect agreement with the result $T_{1/2}(6^+) = 57(5)$ ns obtained from a simple exponential fit in the range outside the prompt region, i.e., for $\Delta t > 100$ ns. To redetermine the half-life of the 8^+ state, the decay curve of the 127.4-keV γ ray was fitted outside the prompt range with a single exponential component, see Fig. 2(c). The resulting half-life of $T_{1/2}(8^+) = 224(4)$ ns is in agreement with the literature values [31,32] but features a significantly reduced uncertainty.

The $B(E2)$ values deduced from the measured half-lives and transition energies, together with the analog information for ^{98}Cd [23], are reported in Table I. Also included are theoretical values of (e_π, e_ν) which were extracted from the measured $B(E2)$ values as detailed below, as well as the predictions from Ref. [8]. We start the discussion considering the most simple valence space, i.e., the one consisting

of a single proton orbital, namely, $\pi 0g_{9/2}$. We find that for both ^{98}Cd and ^{130}Cd , the experimental $B(E2)$ value for the decay of the 8^+ state is well reproduced using a proton effective charge of $e_\pi = 1.5 e$. Note that for two nucleons, or two holes, in a single- j shell, the $B(E2)$ values are independent of the interaction [33]. Considering the full $Z = 28\text{--}50$ major shell as valence space does not alter the above result since the 8^+ , 6^+ , 4^+ levels remain nearly pure $\pi 0g_{9/2}^-$ states.

In the following, LSSM calculations are considered with valence spaces consisting of entire harmonic oscillator shells for both protons and neutrons. For ^{98}Cd , such a $0\hbar\omega$ calculation using the $n = 4$ (sdg) harmonic oscillator shell as valence space was already reported in Ref. [35]. There, the SDGN interaction [37] was used and the excitation of up to five nucleons ($t = 5$) from the $0g_{9/2}$ intruder orbital across the $N = Z = 50$ shell gaps was considered. The effective charges extracted from these calculations are quoted in Table I. In the present work, new $0\hbar\omega$ calculations were performed for ^{130}Cd (again with $t = 5$) considering the $n = 4$ (sdg) and $n = 5$ (pfh) spaces for protons and neutrons, respectively, and using the NNS110 interaction introduced in Ref. [38]. Based on these calculations, effective proton and neutron charges were extracted from the newly measured $B(E2; 8^+ \rightarrow 6^+)$ value in ^{130}Cd and the experimental $B(E2; 6^+ \rightarrow 4^+)$ value in ^{134}Sn [36]. In contrast to the single- j calculations, significant differences between the two Cd isotopes are observed when the ^{100}Sn , respectively, ^{132}Sn cores are opened. In the case of ^{98}Cd , a much smaller proton charge of $e_\pi = 1.11(7)e$ is extracted as compared to the value of $e_\pi = 1.32(2)e$ obtained for ^{130}Cd . The same trend is also observed for the e_π values extracted from the $B(E2; 6^+ \rightarrow 4^+)$ values in $^{98,130}\text{Cd}$ (see Table I), although the latter are systematically larger as compared to those derived from the $8^+ \rightarrow 6^+$ transitions. Such state-dependent effects within the same multiplet, here $\pi 0g_{9/2}^-$, were recently already reported for other heavy nuclei [36,39,40] and will further be discussed in a forthcoming publication [41]. Since their origin is not yet understood, final (e_π, e_ν) values were determined taking into account both these transitions and the $6^+ \rightarrow 4^+$ decays in $^{102,134}\text{Sn}$ [35,36] and the errors of the combined values were multiplied by the square root of the normalized χ^2 . Note that in the LSSM calculations the $t = 0$ content in the relevant wave functions is still about 75%–80% while the remaining 20%–25% are highly fragmented among many different proton and neutron particle-hole configurations. Therefore, it is not to be expected that small variations of the LSSM parametrizations would lead to drastic changes of the extracted effective charges.

The proton and neutron effective charges for the ^{100}Sn and ^{132}Sn cores, extracted from precisely measured transition rates on the basis of $0\hbar\omega$ LSSM calculations, provide

TABLE I. Experimental transition probabilities, $B(E2; I_i^\pi \rightarrow I_f^\pi - 2)$, for transitions in semimagic ^{98}Cd and ^{130}Cd calculated using total internal conversion coefficients from BRICC [34] and proton and neutron effective charges, (e_π, e_ν) , extracted based on single- j and LSSM calculations (see text for details) and predicted by Bohr and Mottelson (BM) [8].

Nucleus	I_i^π	$B(E2)$	Single- j	$0\hbar\omega$ LSSM	
		($e^2 \text{ fm}^4$)	e_π/e	e_π/e	e_ν/e
^{98}Cd	8^+	38.6(41) ^a	1.49(8)	1.11(7) ^b	0.84(2) ^b
	6^+	126(19) ^a	1.70(13)	1.30(11)	
	Combined ^c			1.17(9)	0.83(3)
		BM ^{100}Sn		1.18	0.82
^{130}Cd	8^+	46.2(11)	1.50(2)	1.32(2) ^d	0.54(1) ^d
	6^+	136(7)	1.63(4)	1.45(4)	
	Combined ^e			1.35(5)	0.54(1)
			BM ^{132}Sn	1.05	0.55

^aFrom Ref. [23].

^bFrom Ref. [35].

^c 8^+ and 6^+ decays in ^{98}Cd and 6^+ decay in ^{102}Sn [35].

^d 8^+ decay in ^{130}Cd and 6^+ decay in ^{134}Sn [36].

^e 8^+ and 6^+ decays in ^{130}Cd and 6^+ decay in ^{134}Sn [36].

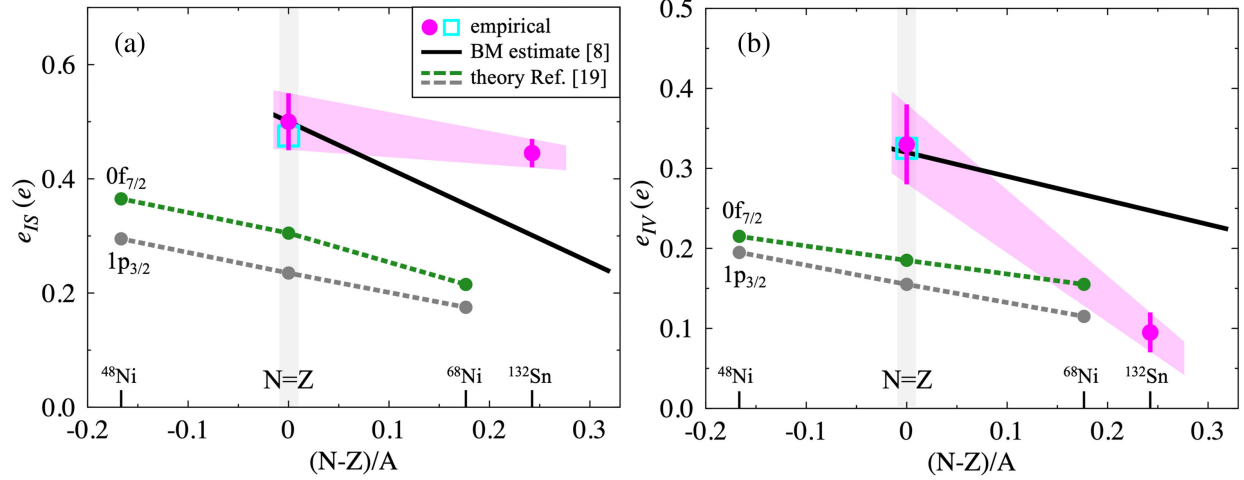


FIG. 3. (a) Isoscalar and (b) isovector effective charges, e_{IS} and e_{IV} , respectively, extracted from experimental data (bullets: $^{100,132}\text{Sn}$ [35] and present work; open square: estimate for ^{56}Ni [21]) as compared to theoretical predictions (black: BM [8], green: $0f_{7/2}$, and gray: $1p_{3/2}$ orbitals from Ref. [19]). The dashed lines and shaded regions are drawn to guide the eye.

the first solid empirical information regarding the isospin dependence of polarization charges in the heavy mass region. The isoscalar, e_{IS} , and isovector, e_{IV} , contributions to the latter arise from virtual excitations of the IS and IV GQR. A first prediction for e_{IS} and e_{IV} and their isospin dependence was made by Bohr and Mottelson many years ago [BM, formula (6-386) of Ref. [8]]. It was derived using the harmonic oscillator model and making several simplifying assumptions. Later on, more elaborate calculations were performed, mainly using the microscopic particle-vibration coupling model based on the Hartree-Fock and random-phase approximations [42–44]. For light nuclei, shell-model calculations including $\Delta n = 2$ single-particle excitations in first order perturbation theory were presented [45]. In a very recent work, orbital-dependent effective charges for several Ni isotopes were calculated from a realistic chiral interaction using *ab initio* approaches [19]. While the authors state that the results for ^{78}Ni may not be fully converged, the calculations for $^{48,56,68}\text{Ni}$ provide a solid microscopically derived prediction of the polarization charges and their isospin dependence in heavy nuclei. In the following, the results reported in the present work will be confronted with both this *ab initio* [19] as well as the BM prediction [8].

As discussed in Ref. [35], the (e_π, e_ν) values extracted for $N = Z$ ^{100}Sn and the region around ^{56}Ni [21] are in very good agreement with the BM prediction. The same is true for the neutron effective charge determined in the present work for ^{132}Sn , while the extracted proton effective charge, $e_\pi = 1.35(5)e$, is significantly larger than the predicted value. Interestingly, the empirical values are close to $e_\pi = 1.31e$, $e_\nu = 0.46e$ calculated by Dufour and Zuker [46] and used in LSSM calculations in the ^{78}Ni region [47,48]. To discuss the isospin dependence of the polarization charges, e_{IS} and e_{IV} (deduced from the relations

$e_\pi = 1 + e_{IS} - e_{IV}$ and $e_\nu = e_{IS} + e_{IV}$) are shown as a function of the relative neutron excess in Fig. 3. The first important observation is that the empirically determined values for the $N = Z$ cores clearly evidence a strong isovector contribution to the polarization charge, as predicted in Ref. [8]. The *ab initio* calculations, in general, yield considerably smaller polarization charges [19]. As representative examples, the results for the $0f_{7/2}$ and $1p_{3/2}$ orbitals are shown in Fig. 3. The new results for the ^{132}Sn core suggest that the isovector charge, e_{IV} , decreases much faster with increasing neutron excess than predicted by the two theoretical approaches. The opposite trend is observed for the isoscalar charge, e_{IS} , which, in contrast to the predictions, barely changes between ^{100}Sn and ^{132}Sn . Note that such a rapid decrease of e_{IV} when leaving the $N = Z$ line, together with a nearly constant e_{IS} , may explain why the effective charges obtained from a fit to available experimental data for the *sd* and *pf* valence spaces seem to indicate rather small isovector contributions (see introduction).

Finally, we mention that the (e_π, e_ν) values chosen “*ad hoc*” to best describe experimental data in recent systematic Monte Carlo shell-model studies of the $^{90-110}\text{Zr}$ [49] and $^{100-138}\text{Sn}$ [50] isotopes, namely, $(1.3e, 0.6e)$ and $(1.25e, 0.75e)$, respectively, are very close to the average over the respective $(N-Z)/A$ ranges considering the isospin dependence empirically established for the Sn isotopes in the present work. It would be very interesting to compare the calculations performed with constant effective charges in Refs. [49,50] to those in which the isospin dependence established here is taken into account.

To conclude, the exotic Cd isotopes in the vicinity of doubly magic ^{100}Sn and ^{132}Sn offer exceptionally clean conditions for the study of the isospin dependence of the proton effective charge due to the existence of seniority

isomers based on the $\pi 0g_{9/2}$ intruder orbital. The precise measurement of the half-lives of the 6^+ and 8^+ states in ^{130}Cd presented here, in combination with available experimental information for ^{98}Cd and new LSSM calculations including the full $0\hbar\omega$ part of the quadrupole operator, allowed us to determine the isospin dependence of the isoscalar and isovector polarization charges. The isovector contribution is shown to decrease much faster with increasing neutron excess than theoretically predicted, while the isoscalar charge stays nearly constant over the full major $N = 50$ – 82 shell. The present work aims to guide the choice of effective charges in future LSSM calculations in the heavy neutron-rich region of the nuclear chart in which experimental information is scarce.

We thank the staff of the RIKEN Nishina Center accelerator complex for providing stable beams with high intensities to the experiment. We acknowledge the EUROBALL Owners Committee for the loan of germanium detectors and the PreSpec Collaboration for the readout electronics of the cluster detectors. This work was supported by MCIN/AEI/10.13039/501100011033, Spain, with Grants No. PID2020–118265 GB-C41 and No. PID2020–118265 GB-C42, the Generalitat Valenciana, Spain, with Grant No. CIPROM/2022/54, EU FEDER funds, and the STFC (UK). P. K. and G. M. P. are supported by the Deutsche Forschungsgemeinschaft (DFG, German Research Foundation)—Project-IDs 448588010, and 279384907—SFB 1245. Zs. V. was supported by NKFIH under projects 2021-4.1.2-NEMZ_KI-2021-00005 and TKP2021-NKTA-42. Work at A. N. L. is supported by the U.S. Department of Energy, Office of Science, Office of Nuclear Physics, under Contract No. DE-AC02-06CH11357.

*Present address: Extreme Light Infrastructure-Nuclear Physics (ELI-NP)/Horia Hulubei National Institute for Physics and Nuclear Engineering (IFIN-HH), Str. Reactorului, Măgurele 077125, Romania.

†Present address: Department of Physics, University of Notre Dame, Notre Dame, Indiana 46556, USA.

- [1] K. Kumar and M. Baranger, *Nucl. Phys.* **A92**, 608 (1967).
- [2] K. Hara and Y. Sun, *Int. J. Mod. Phys. E* **04**, 637 (1995).
- [3] R. F. Casten, *Nuclear Structure from a Simple Perspective*, 2nd ed. (Oxford University Press, New York, 2001).
- [4] K. W. Schmid, *Prog. Part. Nucl. Phys.* **52**, 565 (2004).
- [5] J. Blomqvist and A. Molinari, *Nucl. Phys.* **A106**, 545 (1968).
- [6] M. W. Kirson, *Nucl. Phys.* **A781**, 350 (2007).
- [7] K. Hagino and Y. Maeno, *Found. Chem.* **22**, 267 (2020).
- [8] A. Bohr and B. Mottelson, *Nuclear Structure* (Benjamin, New York, 1975), Vol. 2.
- [9] M. Honma, T. Otsuka, B. A. Brown, and T. Mizusaki, *Phys. Rev. C* **69**, 034335 (2004).
- [10] H. Sagawa and B. A. Brown, *Nucl. Phys.* **A430**, 84 (1984).
- [11] E. Caurier, G. Martínez-Pinedo, F. Nowacki, A. Poves, and A. P. Zuker, *Rev. Mod. Phys.* **77**, 427 (2005).
- [12] W. A. Richter, S. Mkhize, and B. A. Brown, *Phys. Rev. C* **78**, 064302 (2008).
- [13] P. Navrátil, M. Thoresen, and B. R. Barrett, *Phys. Rev. C* **55**, R573(R) (1997).
- [14] I. Hamamoto and H. Sagawa, *Phys. Lett. B* **394**, 1 (1997).
- [15] I. Hamamoto, H. Sagawa, and X. Z. Zhang, *Nucl. Phys.* **A626**, 669 (1997).
- [16] H. L. Ma, B. G. Dong, Y. L. Yan, and X. Z. Zhang, *Phys. Rev. C* **80**, 014316 (2009).
- [17] R. Hoischen, D. Rudolph, H. L. Ma, P. Montuenga, M. Hellström, S. Pietri, Zs. Podolyák, P. H. Regan *et al.*, *J. Phys. G* **38**, 035104 (2011).
- [18] I. Stetcu and J. Rotureau, *Prog. Part. Nucl. Phys.* **69**, 182 (2013).
- [19] F. Raimondi and C. Barbieri, *Phys. Rev. C* **100**, 024317 (2019).
- [20] L. Coraggio, A. Covello, A. Gargano, N. Itaco, and T. T. S. Kuo, *Phys. Rev. C* **91**, 041301(R) (2015).
- [21] R. du Rietz, J. Ekman, D. Rudolph, C. Fahlander, A. Dewald, O. Möller, B. Saha, M. Axiotis *et al.*, *Phys. Rev. Lett.* **93**, 222501 (2004).
- [22] J. J. Valiente-Dobón, D. Mengoni, A. Gadea, E. Farnea, S. M. Lenzi, S. Lunardi, A. Dewald, Th. Pissulla *et al.*, *Phys. Rev. Lett.* **102**, 242502 (2009).
- [23] J. Park, R. Krücken, D. Lubos, R. Gernhäuser, M. Lewitowicz, S. Nishimura, D. S. Ahn, H. Baba *et al.*, *Phys. Rev. C* **96**, 044311 (2017); **103**, 049901(E) (2021).
- [24] T. Kubo, *Nucl. Instrum. Methods Phys. Res., Sect. B* **204**, 97 (2003).
- [25] T. Ohnishi, T. Kubo, K. Kusaka, A. Yoshida, K. Yoshida, M. Ohtake, N. Fukuda, H. Takeda *et al.*, *J. Phys. Soc. Jpn.* **79**, 073201 (2010).
- [26] A. Jungclaus, H. Grawe, S. Nishimura, P. Doornenbal, G. Lorusso, G. S. Simpson, P.-A. Söderström, T. Sumikama *et al.*, *Phys. Rev. C* **94**, 024303 (2016).
- [27] S. Nishimura, *Prog. Theor. Exp. Phys.* **2012**, 03C006 (2012).
- [28] P.-A. Söderström, S. Nishimura, P. Doornenbal, G. Lorusso, T. Sumikama, H. Watanabe, Z. Y. Xu, H. Baba *et al.*, *Nucl. Instrum. Methods Phys. Res., Sect. B* **317**, 649 (2013).
- [29] J. Eberth, H. G. Thomas, P. v. Brentano, R. M. Lieder, H. M. Jäger, H. Kämmerling, M. Berst, D. Gutknecht, and R. Henck, *Nucl. Instrum. Methods Phys. Res., Sect. A* **369**, 135 (1996).
- [30] J. Simpson, *Z. Phys. A* **358**, 139 (1997).
- [31] A. Jungclaus, L. Cáceres, M. Górska, M. Pfützner, S. Pietri, E. Werner-Malento, H. Grawe, K. Langanke *et al.*, *Phys. Rev. Lett.* **99**, 132501 (2007).
- [32] D. Kameda, T. Kubo, T. Ohnishi, K. Kusaka, A. Yoshida, K. Yoshida, M. Ohtake, N. Fukuda *et al.*, *Phys. Rev. C* **86**, 054319 (2012).
- [33] P. J. Brussaard and P. W. M. Glaudemans, *Shell-Model Applications in Nuclear Spectroscopy* (North-Holland, Amsterdam, 1977).
- [34] <http://bricc.anu.edu.au/index.php>.
- [35] H. Grawe, K. Straub, T. Faestermann, M. Górska, C. Hinke, R. Krücken, F. Nowacki, M. Böhmer *et al.*, *Phys. Lett. B* **820**, 136591 (2021).

- [36] M. Piersa-Siłkowska, A. Korgul, J. Benito, L. M. Fraile, E. Adamska, A. N. Andreyev, R. Álvarez-Rodríguez, A. E. Barzakh *et al.*, *Phys. Rev. C* **104**, 044328 (2021).
- [37] M. Górska, *Physics* **4**, 364 (2022).
- [38] H. Naidja, F. Nowacki, and K. Sieja, *Acta Phys. Pol. B* **46**, 669 (2015).
- [39] V. Karayonchev, A. Blazhev, J. Jolie, A. Dewald, A. Esmaylzadeh, C. Fransen, G. Häfner, L. Knafla *et al.*, *Phys. Rev. C* **106**, 044321 (2022).
- [40] R. Broda, L. W. Iskra, R. V. F. Janssens, B. A. Brown, B. Fornal, J. Wrzesiński, N. Cieplicka-Oryńczak, M. P. Carpenter *et al.*, *Phys. Rev. C* **98**, 024324 (2018).
- [41] M. Armstrong *et al.* (to be published).
- [42] I. Hamamoto and H. Sagawa, *Phys. Lett. B* **394**, 1 (1997).
- [43] H. Sagawa and K. Asahi, *Phys. Rev. C* **63**, 064310 (2001).
- [44] H. Sagawa, X. R. Zhou, X. Z. Zhang, and T. Suzuki, *Phys. Rev. C* **70**, 054316 (2004).
- [45] A. Umeya, G. Kaneko, and K. Muto, *Nucl. Phys. A* **829**, 13 (2009).
- [46] M. Dufour and A. P. Zuker, *Phys. Rev. C* **54**, 1641 (1996).
- [47] F. Nowacki, A. Poves, E. Caurier, and B. Bounthong, *Phys. Rev. Lett.* **117**, 272501 (2016).
- [48] R. Taniuchi, C. Santamaria, P. Doornenbal, A. Obertelli, K. Yoneda, G. Authelet, H. Baba, D. Calvet *et al.*, *Nature (London)* **569**, 53 (2019).
- [49] T. Togashi, Y. Tsunoda, T. Otsuka, and N. Shimizu, *Phys. Rev. Lett.* **117**, 172502 (2016).
- [50] T. Togashi, Y. Tsunoda, T. Otsuka, N. Shimizu, and M. Honma, *Phys. Rev. Lett.* **121**, 062501 (2018).